Signaling adaptor ShcD suppresses extracellular signal-regulated kinase (Erk) phosphorylation distal to the Ret and Trk neurotrophic receptors

Melanie K. B. Wills[‡1], Ava Keyvani Chahi[‡2], Hayley R. Lau[‡2,3], Manali Tilak[‡2,4], Brianna D. Guild[‡5], Laura A. New[‡], Peihua Lu[‡], Kévin Jacquet[§6], Susan O. Meakin[¶], Nicolas Bisson[§], and Nina Jones[‡7]

From the ‡Department of Molecular and Cellular Biology, University of Guelph, Guelph, Ontario N1G 2W1, Canada, §Cancer Research Centre, Quebec Network for Research on Protein Function, Engineering, and Applications (PROTEO) and Centre Hospitalier de Québec Research Centre-Université Laval, Québec City, Québec G1R 2J6, Canada, and ¶Department of Biochemistry, Western University, London, Ontario N6A 5B7, Canada

Edited by Alex Toker

Proteins of the Src homology and collagen (Shc) family are typically involved in signal transduction events involving Ras/MAPK and PI3K/Akt pathways. In the nervous system, they function proximal to the neurotrophic factors that regulate cell survival, differentiation, and neuron-specific characteristics. The least characterized homolog, ShcD, is robustly expressed in the developing and mature nervous system, but its contributions to neural cell circuitry are largely uncharted. We now report that ShcD binds to active Ret, TrkA, and TrkB neurotrophic factor receptors predominantly via its phosphotyrosine-binding (PTB) domain. However, in contrast to the conventional Shc adaptors, ShcD suppresses distal phosphorylation of the Erk MAPK. Accordingly, genetic knock-out of mouse ShcD enhances Erk phosphorylation in the brain. In cultured cells, this capacity is tightly aligned to phosphorylation of ShcD CH1 region tyrosine motifs, which serve as docking platforms for signal transducers, such as Grb2. Erk suppression is relieved through independent mutagenesis of the PTB domain and the CH1 tyrosine residues, and successive substitution of these tyrosines breaks the interaction between ShcD and Grb2, thereby promoting TrkB-Grb2 association. Erk phosphorylation can also be restored in the presence of wild type ShcD through Grb2 overexpression. Conversely, mutation of the ShcD SH2 domain results in enhanced repression of Erk. Although the SH2 domain is a less common binding interface in Shc proteins, we demonstrate that it associates with the Ptpn11

(Shp2) phosphatase, which in turn regulates ShcD tyrosine phosphorylation. We therefore propose a model whereby ShcD competes with neurotrophic receptors for Grb2 binding and opposes activation of the MAPK cascade.

Signal transduction is a vital process whereby external stimuli direct the physiological activity of individual cells in an organism. The underlying biochemical networks are built around a multitude of enzymatic components, such as receptor tyrosine kinases (RTKs),[8] in addition to non-catalytic adaptor proteins like those of the Src homology and collagen (Shc) family, which serve as scaffolds for the developing signaling complex (1). Four Shc paralogs have been described in mammals, commonly designated Shc/ShcA/Shc1, ShcB/Sck/Shc2, ShcC/N-Shc/Rai/Shc3, and ShcD/RaLP/Shc4 in chronological order of their discovery (2). They share a conserved architecture consisting of an amino-proximal phosphotyrosine-binding (PTB) domain, a carboxyl-terminal Src homology 2 (SH2) domain, and two collagen homology regions designated CH1 and CH2. The PTB and SH2 domains connect the adaptor to activated plasma membrane receptors, including those for growth factors, cytokines, and extracellular matrix, whereas the central CH1 region is enriched in phosphorylatable tyrosine residues that recruit additional signal transducers, such as Grb2, into the developing complex (2) (depicted in Fig. 1D).

ShcA is the best characterized and most ubiquitous member of the family with the exception of the mature nervous system in which it is restricted to neurogenic regions (3). In contrast, ShcB and -C are almost exclusively expressed in neurons of the central and peripheral nervous systems (4), although ShcC has also been described in enteric glial cells (5) and lymphocytes (6,

7). ShcD has likewise been identified throughout the adult brain and to a lesser extent in skin and muscle (8–10).

Despite their conserved structure and common binding partners, the Shc adaptors and their isoforms can give rise to distinct downstream signals and make unique physiological contributions. The most striking example of this phenomenon is the functional disparity between the canonical p46/p52 ShcA isoforms, which augment transduction events at the membrane, and p66 ShcA, which functions as a mitochondrial redox sensor that contributes to apoptosis (11). The three isoforms differ only in the length of their amino-terminal CH2 regions (12, 13). Shc non-redundancy is also evident in the developing nervous system where a molecular switch demarcates progenitor cell proliferation and terminal differentiation. During the transition, levels of ShcA decrease, whereas ShcC increases and achieves maximal expression in postmitotic neurons (14). ShcC appears to support survival and maturation through specific engagement of the phosphatidylinositol 3-kinase (PI3K)/Akt pathway and prolonged activation of Erk1/2 (p44/p42) mitogen-activated protein kinase (MAPK), respectively (14).

In the nervous system, such responses are elicited by the class of signaling ligands known as neurotrophic factors. Together with their companion receptors, these factors support neurons during development and through maturity, influencing common cellular characteristics like survival while also guiding specialized functions, such as axonal pathfinding and synaptic plasticity (15). Two prominent families in this growth factor class are the neurotrophins and their corresponding tropomyosin-related kinase (Trk) RTKs and the glial cell line-derived neurotrophic factor family ligands with their multicomponent receptor consisting of the rearranged during transformation (Ret) RTK and one of four ligand-specific glial cell line-derived neurotrophic factor family receptor α co-receptors (16, 17). Collectively, neurotrophic signaling has far reaching implications in organism morphogenesis, maintenance, and a spectrum of diseases, including Alzheimer's, depression, inflammatory pain, and cancer (18). Understanding the signaling networks that underlie aberrant behavior is therefore a priority.

To that end, ShcA, -B, and -C bind Trk and Ret RTKs and augment Ras/MAPK and/or PI3K/Akt signaling (19–21). Little is known of the neuronal contributions of the recently discovered ShcD, although its potential to bind activated Ret and Trk was revealed in a high-throughput peptide screen (22), and associations with TrkB have been demonstrated *in vitro* (23). We have previously shown that ShcD elicits ligand-independent phosphorylation of the epidermal growth factor (EGF) receptor (EGFR) (24) and promotes its accumulation in juxtanuclear endocytic recycling compartments,[9] thereby establishing a precedent for non-canonical engagement of ShcD in signaling circuitry. We now report that ShcD suppresses Erk activation in the context of Ret, TrkA, and TrkB. Further investigation with TrkB revealed that the phenotype arises from Grb2 sequestration and that the Ptpn11 (Shp2) phosphatase regulates CH1 region phosphotyrosine residues to oppose this phenomenon. ShcD thus appears to function as a signaling platform that facilitates negative regulation of Erk.

Results

Ret, TrkA, and TrkB bind ShcD predominantly via its PTB domain

Because of the robust expression of ShcD in the nervous system (8, 9), we set out to investigate findings from our peptide screen suggesting that the adaptor binds to Ret and Trk neurotrophic receptors (22). To this end, we introduced the oncogenic Ret MEN2A receptor (kinase-active) or its kinase-dead (KD) counterpart into human embryonic kidney (HEK) 293T cells along with ShcD to assess protein-protein interactions by way of immunoprecipitation. Ret MEN2A is characterized by a point mutation in the extracellular region that promotes homodimerization and autoactivation (25), and we first confirmed that the kinase was indeed constitutively active in our expression system (Fig. 1*A*). Tyrosine phosphorylation of the receptor was found to be required for Ret-ShcD association (Fig. 1*A*) as suggested previously by the peptide array (22).

We next confirmed that overexpression of the wild type TrkA and TrkB receptors in HEK 293T cells was sufficient to promote their tyrosine phosphoactivation (Fig. 1, *B* and *C*, *fourth panel*). ShcD and the positive control, ShcA, were each independently able to bind the wild type TrkA and TrkB receptors, but neither adaptor co-precipitated the kinase-dead variant, thereby implicating tyrosine phosphorylation as a prerequisite for association (Fig. 1, *B* and *C*).

To identify regions of ShcD that mediate its interactions with neurotrophic receptors, we subsequently introduced ShcD mutants containing a disabled PTB domain (PTB*), SH2 domain (SH2*), or tandem tyrosine-to-phenylalanine substitutions in the CH1 region (Y374F/Y375F/Y403F/Y413F/Y424F/Y465F (Y6F)) (depicted schematically in Fig. 1*D*) with the RTKs. Disrupting the tyrosine-binding functionality of the ShcD PTB domain substantially impeded co-precipitation of all three RTKs, whereas the SH2 domain was a minor factor in the interaction (Fig. 1, *E*, *F*, and *G*). Compound ablation of both domains elicited the most profound loss of receptor-adaptor association. By contrast, the ShcD Y6F variant retained the full Ret-, TrkA-, and TrkB-binding capacities of wild type ShcD (Fig. 1, *E*, *F*, and *G*). Thus, the PTB domain appears to be the primary point of contact between neurotrophin receptors and ShcD with some additional influence of the SH2 domain.

ShcD opposes Erk activation downstream of Ret and Trk receptors

Although traditional Shc adaptors are well established mediators of MAPK signaling, the contribution of ShcD to canonical pathways has been less clear (24). We therefore profiled Akt and Erk phosphorylation in response to active neurotrophic receptors co-expressed with ShcD variants. Proximal to Ret, TrkA, and TrkB, wild type ShcD was itself found to be phosphorylated in keeping with the canonical response of Shc family proteins (Fig. 2). It nevertheless failed to influence Akt, which maintained the same degree of phosphorylation across the panel of conditions and ShcD mutants tested (Fig. 2, *A*, *B*, and *C*). Surprisingly, however, wild type ShcD attenuated Erk1/2 phosphorylation (pErk) distal to all three receptors (Fig. 2, *A*, *B*, and *C*), and with each RTK, pErk levels were restored in the
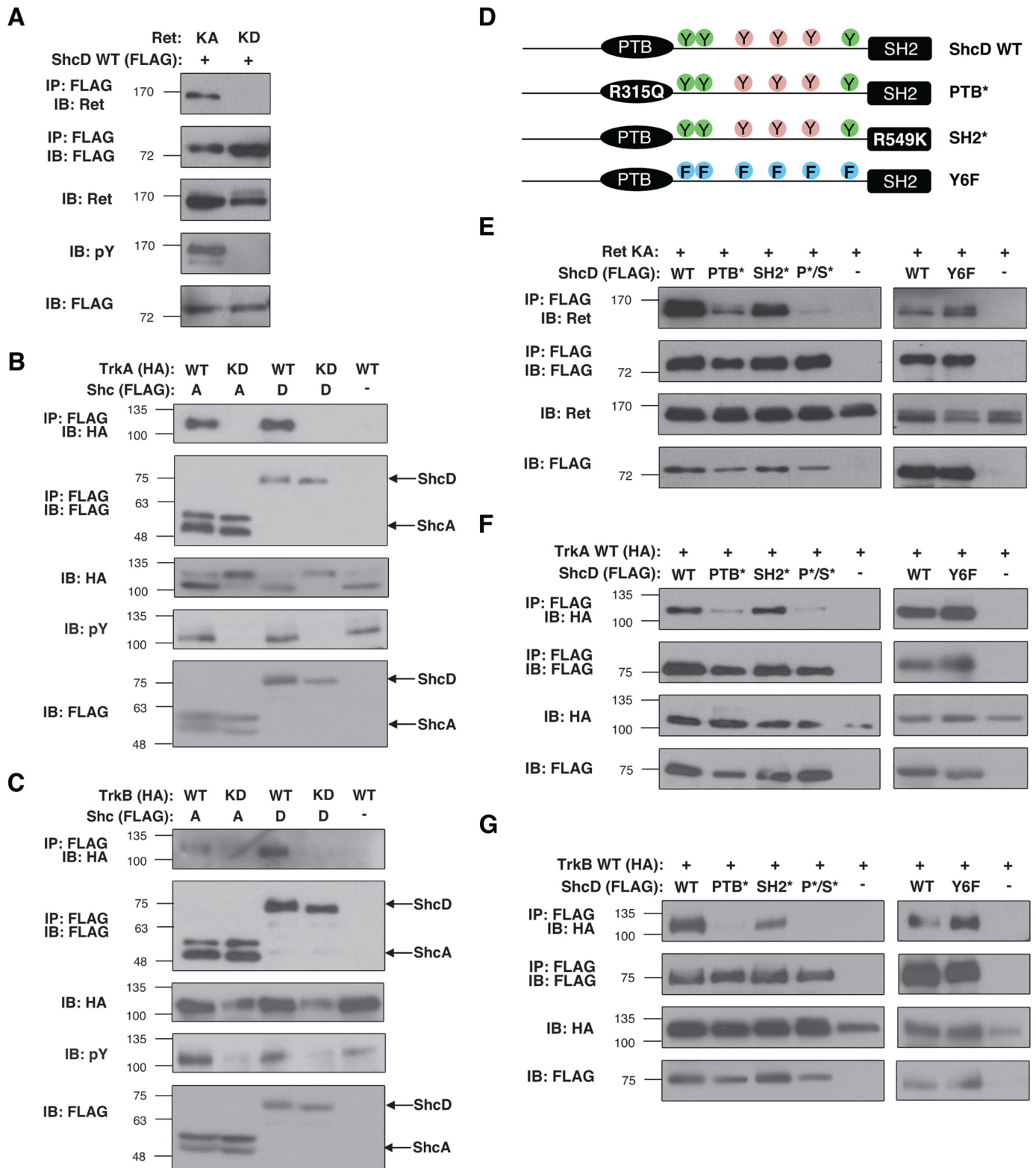
Figure 1. The ShcD PTB domain is the principal point of contact with Ret, TrkA, and TrkB. *A*, lysates from HEK 293T cells transiently expressing ShcD-FLAG with Ret MEN2A or the KD variant (K758M) were FLAG-immunoprecipitated and immunoblotted to detect Ret. Receptor tyrosine phosphorylation was required to establish an interaction with ShcD. *B* and *C*, similarly, ShcA and ShcD were co-expressed with wild type or kinase-dead TrkA-HA and TrkB-HA (TrkA KD, K547A; TrkB KD, K573A) and subjected to co-immunoprecipitations that confirmed the importance of receptor catalytic activity in enabling associations with Shc. *D*, schematic representations of ShcD depicting the PTB and SH2 domains as well as the CH1 region tyrosine residues of which those in *green* are conserved across the family. Also shown are strategic point mutations that disable the functions of each of these components. *E*, *F*, and *G*, wild type Ret, TrkA, or TrkB were co-immunoprecipitated with wild type and mutant ShcD. Disabling the ShcD PTB domain had the most profound influence on receptor binding, and no effects were seen with the Y6F mutant. *KA*, kinase active; *IP*, immunoprecipitation; *IB*, immunoblot; *pY*, phosphotyrosine; *P*/S**, ShcD PTB*/SH2* compound mutant.
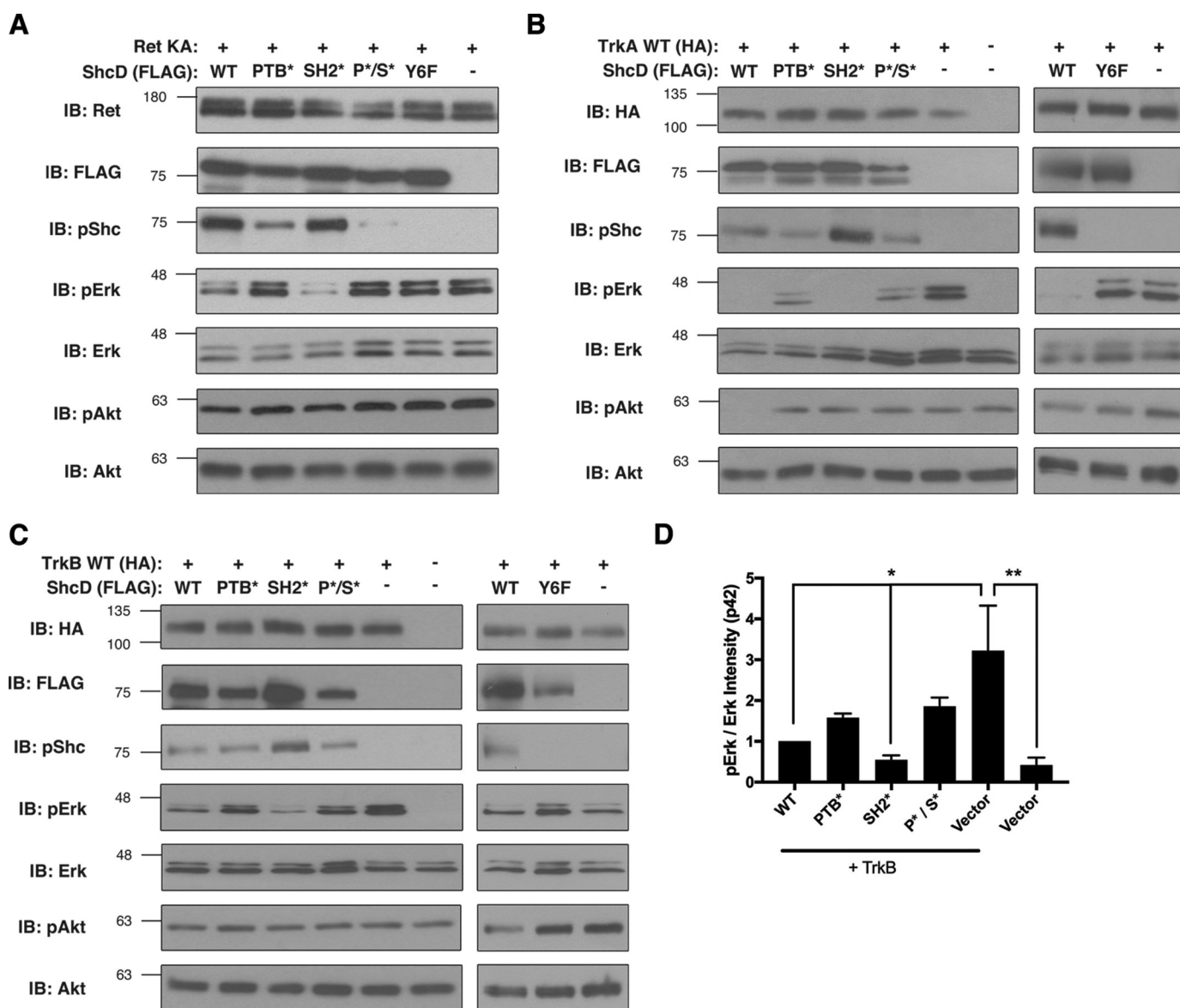
Figure 2. ShcD suppresses Erk phosphorylation proximal to neurotrophic receptors. The same ShcD-FLAG mutants used in Fig. 1 were assessed for their Akt and Erk signaling potential in the context of Ret MEN2A (*A*), TrkA-HA (*B*), and TrkB-HA (*C* and *D*). In each case, wild type and SH2* ShcD were themselves robustly phosphorylated while repressing Erk activation, whereas the PTB* and Y6F mutants had little to no phosphorylation and permitted MAPK activation. *D*, densitometric analysis of TrkB immunoblot band intensities is expressed as a ratio of pErk/Erk relative to wild type ShcD. Repeated measures one-way ANOVA ($n = 4$; $p = 0.0066$) followed by Tukey's multiple comparison test revealed a significant difference between the ShcD-negative sample (*Vector*) and each of ShcD WT and ShcD SH2*. Multiplicity-adjusted p values are as follows: ShcD WT *versus* vector, $p = 0.0385$; SH2* *versus* vector, $p = 0.0104$; vector (+TrkB) *versus* vector (−Trk), $p = 0.0071$. *Error bars* denote S.E. *, $p \leq 0.05$; **, $p \leq 0.01$. *IB*, immunoblot; *KA*, kinase-active; *P*/S**, ShcD PTB*/SH2* compound mutant.

presence of the ShcD PTB*, PTB*/SH2*, and Y6F mutants. Notably, ShcD SH2* appeared to function as a super-repressor, reducing phosphorylated Erk below the levels generated downstream of wild type ShcD (quantitated in Fig. 2*D*).

ShcD knock-out increases pErk in the murine brain

To better understand the physiological extent of ShcD influence over Erk, we turned to our recently generated whole body ShcD knock-out mice, which are viable and appear normal in gross morphology.[10] As our previous work revealed robust ShcD expression throughout the developing and adult brain (8, 9), we focused on this organ to identify changes arising from

ShcD removal. In brain homogenate prepared from mice, we observed a reduction in ShcD protein in heterozygous animals compared with wild type (WT) littermates and complete elimination in full knock-outs (KOs) (Fig. 3*A*). Remarkably, ShcD control of pErk was also seen *in vivo* where the loss of ShcD resulted in Erk hyperactivation (Fig. 3*B*). Quantitation of the phenomenon revealed a mean 2-fold increase in the pErk/Erk ratios when comparing the ShcD KO brain with that of WT controls (Fig. 3*C*).

ShcD suppresses Erk phosphorylation by sequestering Grb2

Our unexpected discovery that ShcD reduces Erk output in cultured cells and in the mouse model prompted further mechanistic characterization of this response. As depicted in Fig. 2,

---

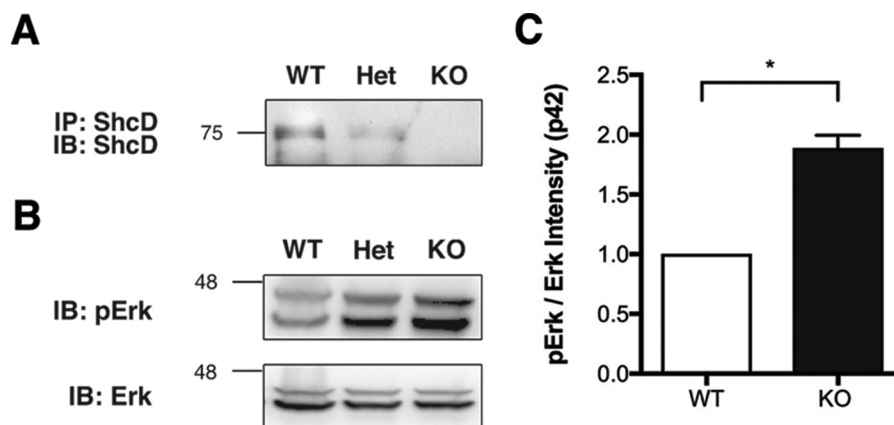[10] L. A. New, H. N. Robeson, and N. Jones, manuscript in preparation.

Figure 3. ShcD knock-out enhances pErk in mouse brain. *A*, whole brains of wild type, ShcD$^{+/-}$ heterozygous, and ShcD-null mice were assayed by immunoprecipitation and immunoblotting for the presence of ShcD protein. ShcD expression was reduced in heterozygous mice and absent from knock-out animals. *B*, brain lysates were further analyzed for pErk and Erk by immunoblotting. *C*, densitometry showing that removal of ShcD was associated with a 2-fold increase in p42 Erk phosphorylation ($n = 3$; $p = 0.0265$ by paired *t* test). *Error bars* denote S.E. *, $p \leq 0.05$. *Het*, heterozygote; *KO*, knock-out (genetic ShcD-null); *IP*, immunoprecipitation; *IB*, immunoblot.

the distinct ShcD mutations that rescued Erk phosphorylation are similar in that they disable the phosphotyrosine transduction capacity of the adaptor either by physically uncoupling ShcD from the stimulated receptor (PTB* and PTB*/SH2*) or by preventing it from recruiting proximal effectors (Y6F). Indeed, the Erk activation pattern appeared to be reciprocal to the ShcD phosphorylation status such that decreased pShc was associated with increased pErk (Fig. 2, *A*, *B*, and *C*). Considering that Grb2 is the major canonical binding partner of the ShcD tyrosine residues (9), we questioned whether the signaling output was influenced by sequestration of this adaptor. Because all three neurotrophic receptors demonstrated identical Erk activation and repression patterns in concert with ShcD and its mutants, we proceeded to characterize the response using TrkB as a model. We first evaluated the extent of interaction between endogenous Grb2 and wild type or domain-mutated ShcD. Consistent with our hypothesis, PTB*, but not SH2*, prevented co-precipitation of Grb2 with ShcD (Fig. 4*A*). To pursue the impact of ShcD CH1 tyrosine residue loss, we introduced successive phenylalanine substitutions as depicted in the schematic in Fig. 4*B*. Removal of ShcD tyrosines 374/375 (Y374F/Y375F (Y2F)) completely abolished reactivity to the pShc antibody, which was raised against equivalent residues 239/240 of p52 ShcA (Fig. 4*C*). As predicted, incremental loss of ShcD tyrosine motifs promoted Erk phosphorylation with the most dramatic shift occurring between Y3F and Y4F (Fig. 4*D*) in which all known Grb2 recognition sites have been removed (depicted in *green* in Fig. 4*B*). Tyrosine 424, which is absent in ShcD Y4F, was identified previously as a novel Grb2 motif unique to ShcD (9). The additional substitution of two other non-consensus tyrosine residues (Tyr-403 and Tyr-413; ShcD Y6F) did not contribute to the phospho-Erk response (Fig. 4, *C* and *D*). It would therefore appear that ShcD Tyr-374/375, Tyr-424, and Tyr-465 are major mediators of Erk repression. To evaluate the role of Grb2 in this response, we monitored interactions between ShcD-Grb2 and TrkB-Grb2 by co-immunoprecipitations across the series of tyrosine-to-phenylalanine mutants. ShcD Y2F demonstrated a profound loss of endogenous Grb2 binding, and the association appeared to be fully

abolished by the additional ShcD Y465F substitution (Y3F; Fig. 4*C*). Correspondingly, TrkB-Grb2 binding increased as the ShcD-Grb2 interaction decreased (Fig. 4*C*).

Collectively, these observations demonstrate that differential partitioning of Grb2 between ShcD and TrkB correlates with Erk phosphorylation status. They also suggest that endogenous Grb2 is a limiting reagent in the context of overexpressed binding partners, which establishes competition between TrkB and ShcD for the available pool. To address this hypothesis, we overexpressed Grb2 in combination with TrkB and either wild type, PTB*, or SH2* ShcD. As depicted in Fig. 4*E*, pErk levels varied predictably between the ShcD permutations prior to the addition of exogenous Grb2. Introducing Grb2 equalized Erk phosphorylation among samples expressing wild type ShcD, PTB*, and SH2* (Fig. 4*E*). It also had the effect of markedly enhancing ShcD phosphorylation without affecting overall protein levels. Thus, it would appear that overexpressed, wild type ShcD can sequester Grb2 away from MAPK-directed outcomes. In this regard, Grb2 appears to assume opposing roles depending on whether it is directly or indirectly recruited into the signaling complex.

Shp2 binds ShcD and regulates CH1 region tyrosine phosphorylation and Erk response

Another striking and unexplained characteristic of the ShcD signaling response is the capacity of the SH2* mutant to act as a super-repressor of Erk. ShcD SH2* binds the activated receptor (Fig. 1) and is phosphorylated to a greater extent than the wild type protein (Fig. 2) in keeping with the observation that pShc status inversely correlates with pErk outcome. This implied the possible engagement of a regulatory component, such as a phosphatase, via the functional ShcD SH2 domain. To that end, we used affinity purification-mass spectrometry to survey proteins associated with ShcD and identified the Shp2 phosphatase as a putative binding partner. This interaction was confirmed by co-immunoprecipitations performed in the presence and absence of TrkB, which demonstrated a robust association between ShcD and Shp2 under both conditions (Fig. 5*A*). Notably, the introduction of Shp2 was found to enhance levels of
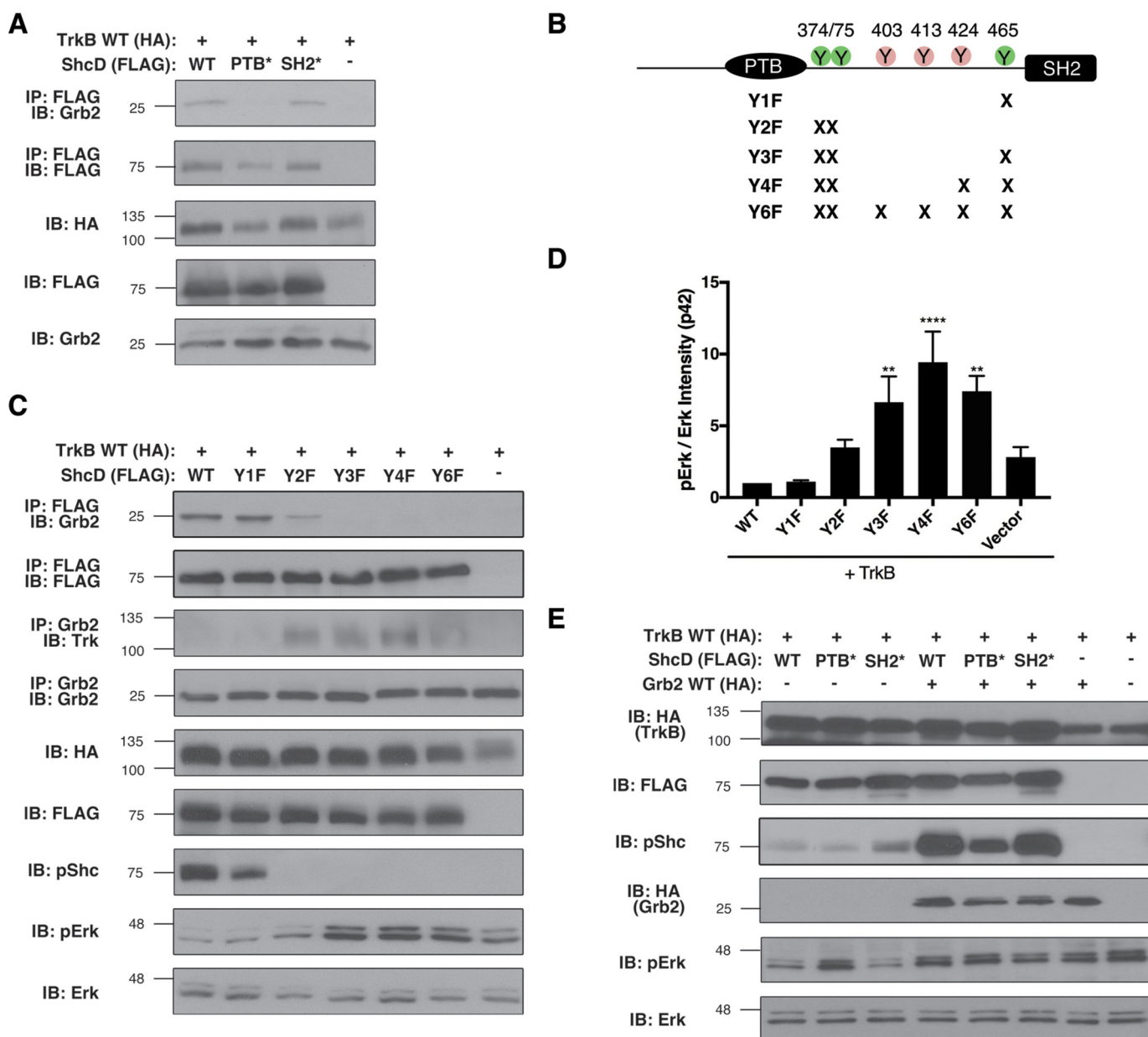
Figure 4. ShcD sequesters Grb2 to reduce Erk activation. *A*, the capacity of transfected wild type ShcD-FLAG and its tyrosine-binding mutants to co-precipitate endogenous Grb2 was assessed in the presence of TrkB-HA. Disabling the ShcD PTB domain, but not the SH2 domain, impeded the ShcD-Grb2 association. *B*, schematic representation of tyrosine-to-phenylalanine point mutations in ShcD that successively eliminate phosphomotifs. *Green* residues are conserved across the Shc family, whereas *peach* residues are unique to ShcD. Tyr-374/375, Tyr-465, and Tyr-424 are validated Grb2-binding sites. *C*, incremental ShcD tyrosine losses were assessed for their impact on three parameters: ShcD-Grb2 binding, TrkB-Grb2 binding, and pErk signaling output. Transitioning from wild type ShcD through Y6F abolished the ShcD-Grb2 association, enhanced TrkB-Grb2, and increased pErk. *D*, densitometry corresponding to *C* is expressed as a ratio of pErk/Erk relative to ShcD WT. Values were analyzed by repeated measures one-way ANOVA ($n = 5$; $p < 0.0001$) followed by Tukey's multiple comparison test. Multiplicity-adjusted p values for each significant pair are as follows: WT *versus* Y3F, $p = 0.0056$; WT *versus* Y4F, $p < 0.0001$; WT *versus* Y6F, $p = 0.0014$; Y1F *versus* Y3F, $p = 0.0068$; Y1F *versus* Y4F, $p < 0.0001$; Y1F *versus* Y6F, $p = 0.0017$; Y2F *versus* Y4F, $p = 0.0033$; Y4F *versus* vector, $p = 0.0010$; Y6F *versus* vector, $p = 0.0336$. *Error bars* denote S.E. *E*, to evaluate whether ShcD was quenching pErk by sequestering the cellular pool of Grb2, we overexpressed Grb2-HA in the presence of ShcD and select mutants. This was sufficient to reverse Erk suppression caused by wild type ShcD and the more potent SH2* mutant. **, $p \leq 0.01$; ****, $p \leq 0.0001$. *IP*, immunoprecipitation; *IB*, immunoblot.

TrkB and ShcD proteins while concomitantly reducing ShcD phosphorylation.

When we extended the binding analysis to ShcD variants, we discovered that the SH2* mutation in the full-length ShcD protein profoundly disrupted the Shp2 interaction (Fig. 5*B*) as anticipated under our hypothesis. This was further verified by GST pulldown analyses involving the individual ShcD domains incubated with lysate containing Shp2 in the presence or

absence of TrkB. Here, the addition of the RTK was found to strengthen the association between Shp2 and the isolated ShcD SH2 domain (Fig. 5*C*). Although not as dramatic, the ShcD Y6F substitutions also reproducibly reduced ShcD-Shp2 binding (Fig. 5*B*).

Considering that Shp2 appears to suppress ShcD phosphorylation, which we have demonstrated is correlated with enhanced pErk signaling, we questioned whether Shp2 overex-

pression could rescue Erk phosphorylation. Indeed, introducing Shp2 in concert with TrkB and wild type ShcD promoted a substantial increase in pErk signal coincident with reduced pShc (Fig. 5D). These phenomena could not be recapitulated with the dominant-negative substrate-trapping Shp2 Cys-to-Ser mutant, which had the opposite effect of boosting ShcD phosphorylation and further suppressing pErk (Fig. 5, D and E).

Moreover, wild type Shp2 partially restored Erk phosphorylation in the context of the super-repressor, ShcD SH2*, even though the principal Shp2 interaction motif was absent. Taken together, our results suggest that ShcD is both a binding partner and a functional target of Shp2 and that the consequences of this association manifest in the MAPK pathway. The overall signaling outcomes thus appear to be the product of several
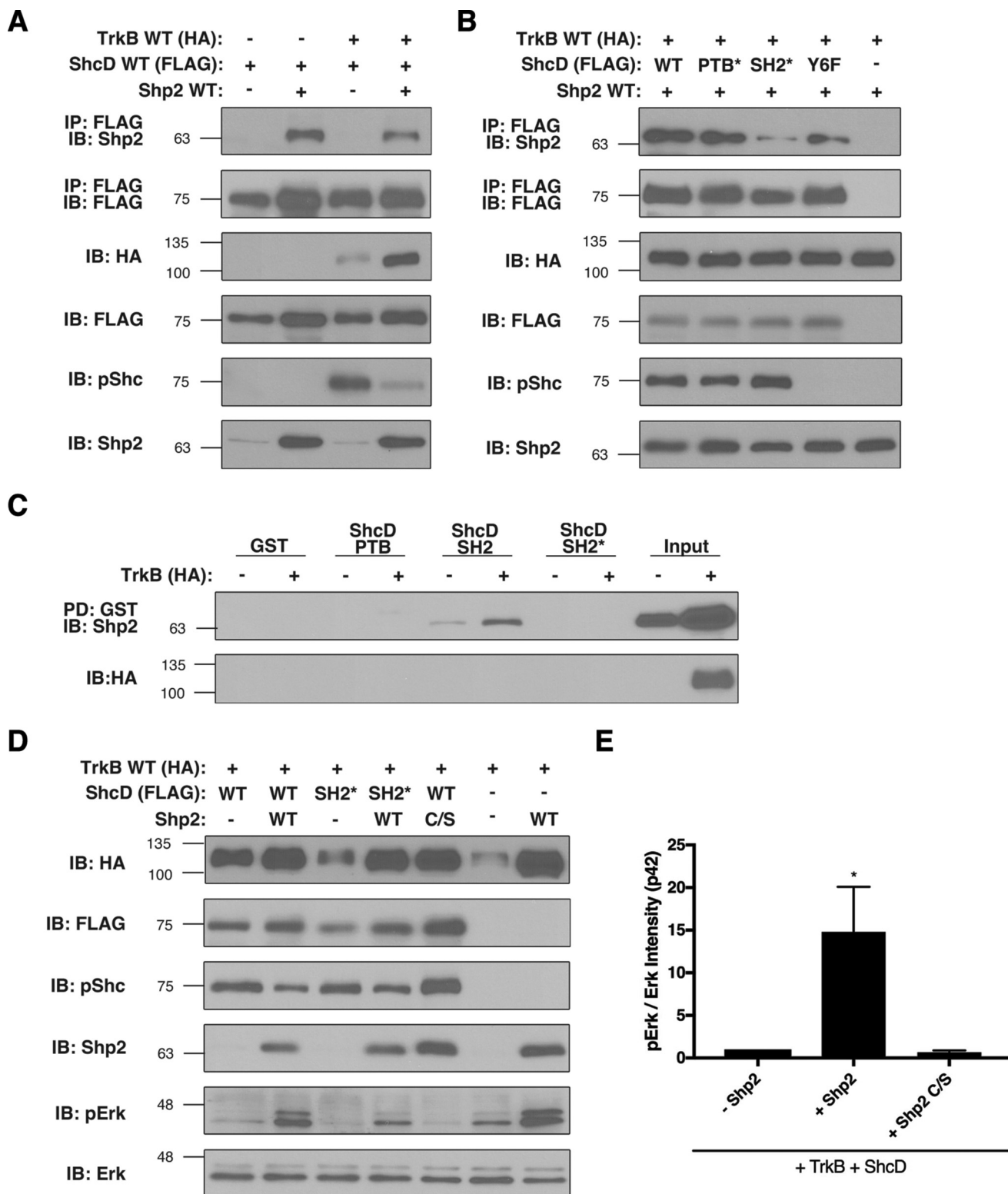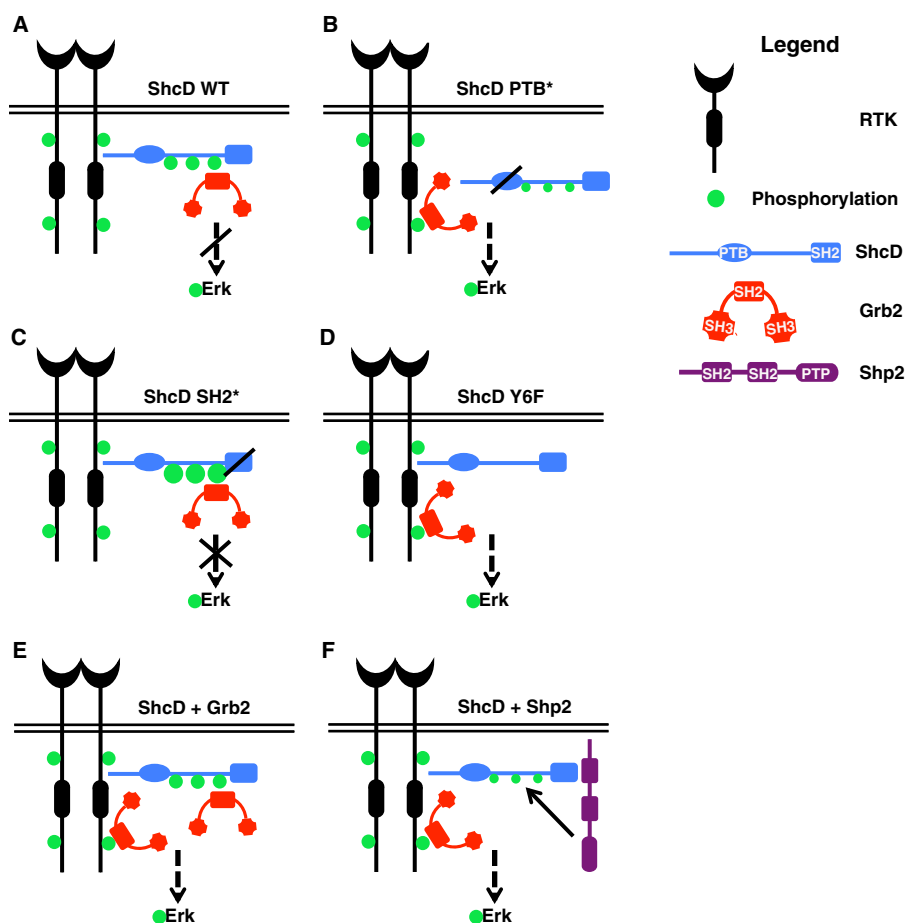
Figure 6. Schematic representations of ShcD-mediated Erk repression and circumstances conferring rescue. The resulting model derived from our findings posits that RTK-Grb2 associations formed in the absence of ShcD augment distal Erk phosphorylation, whereas recruitment of Grb2 (*red*) via ShcD (*blue*) phosphomotifs (*green*) renders it less capable of activating the MAPK cascade. *A*, accordingly, when Grb2 protein levels are lower than those of plasmid-expressed TrkB and ShcD, pShcD adsorbs and sequesters a substantial portion of the available Grb2, thereby inhibiting Erk activation. Reducing ShcD phosphorylation by disconnecting the adaptor from the receptor (PTB*) (*B*) or removing sites of modification (Y6F) (*D*) rescues pErk. *C*, meanwhile, the highest degree of ShcD phosphorylation is achieved when the SH2 domain is disabled and incapable of binding the Shp2 phosphatase, and this corresponds to the most extensive pErk quenching. Overexpression of either Grb2 (*E*) or Shp2 (*purple*) (*F*) in the presence of ShcD restores Erk phosphorylation.

factors, including ShcD phosphorylation status and the availability of Grb2 and Shp2 in the cell, as illustrated in Fig. 6.

Discussion

Ras/MAPK pathway activation was the first signaling outcome attributed to Shc, and it remains the best characterized classical response of this protein family (2). Nevertheless, exceptions to this paradigm do exist, and we describe here the first detailed account of ShcD-mediated repression of Erk phosphorylation. Our findings suggest that, although ShcD is recruited via its PTB domain to active Ret and Trk, it does not function as a canonical adaptor linking these receptors to the MAPK cascade but instead regulates the engagement of other pathway componentry to sculpt the signaling output.

As depicted in Fig. 6, the capacity of transfected ShcD to suppress Erk phosphorylation distal to the neurotrophic receptors is tightly coupled to its CH1 region tyrosine phosphorylation status. Grb2 is both a central node in the Ras/MAPK pathway and the canonical binding partner of three ShcD phosphotyrosine motifs (9), and our work suggests that it is the com-

Figure 5. Shp2 binds the ShcD SH2 domain and regulates CH1 region tyrosine phosphorylation, influencing distal signaling. *A*, the potential for Shp2 to associate with ShcD was first pursued via co-immunoprecipitation analyses from cells transfected with a combination of TrkB-HA, ShcD-FLAG, and Shp2. An ShcD-Shp2 interaction was detected in the presence and absence of the RTK, and Shp2 was found to oppose TrkB-mediated ShcD phosphorylation. *B*, to determine the Shp2 docking site on ShcD, the PTB*, SH2*, and Y6F ShcD mutants were co-expressed with TrkB-HA and Shp2. ShcD-FLAG immunoprecipitation followed by Shp2 immunoblotting demonstrated that disabling the ShcD SH2 domain reduced Shp2 binding. *C*, to further validate the interaction, GST fusions of the isolated PTB, SH2, and SH2* domains of ShcD were incubated with glutathione beads and cell lysates from Shp2 alone or Shp2 + TrkB-HA-transfected cells. The wild type ShcD SH2 domain successfully co-precipitated Shp2 with a stronger association noted in the presence of TrkB. Interactions with Shp2 were substantially reduced by the SH2* mutant. *D*, to confirm the effects of Shp2 on ShcD phosphorylation, wild type or SH2* ShcD was coexpressed with TrkB-HA with and without Shp2 wild type or dominant-negative Cys-to-Ser (*C/S*) mutants. ShcD phosphorylation decreased in the presence of Shp2 and increased with the Cys-to-Ser mutant. Conversely, Erk activation was higher in the presence of Shp2 and substantially reduced with the Cys-to-Ser mutant, demonstrating that Shp2 positively regulates Erk activation by dephosphorylating ShcD. *E*, pErk/Erk intensity ratios relative to ShcD WT as determined from immunoblot densitometry performed on *D* confirm the visual observations. One-way ANOVA ($n \geq 3$; $p = 0.0152$) followed by Tukey's multiple comparison test yielded the following multiplicity-adjusted p values for significant pairs: −Shp2 *versus* +Shp2, $p = 0.0206$; +Shp2 *versus* +Shp2 Cys-to-Ser, $p = 0.0349$. *Error bars* denote S.E. *, $p \leq 0.05$. *IP*, immunoprecipitation; *PD*, pulldown; *IB*, immunoblot.

mon factor responsible for the signaling outcomes observed. Under this model, tyrosine-phosphorylated ShcD serves as a multivalent vehicle for Grb2 that competes with other consensus motifs to recruit the adaptor and subsequently reduces Grb2 engagement in the MAPK cascade. The major variable that determines signaling output thus appears to be the pShcD: Grb2 ratio, which establishes differential Grb2 partitioning between the RTK and ShcD. Accordingly, exogenous Grb2 mitigates the signaling consequences of ShcD while concomitantly enhancing pShcD, which implies that it is not Shc phosphorylation *per se* that drives the signaling phenotype but rather the capacity of the adaptor to regulate the cellular pool of Grb2. In this regard, overexpressing Grb2 saturates the system to promote Erk phosphorylation, whereas the opposite strategy of introducing Shp2 phosphatase elicits the same ultimate response by decreasing ShcD phosphorylation and/or promoting turnover at the Grb2 consensus motifs, thereby increasing the cytosolic availability of Grb2 (Fig. 6F).

The significance of this free pool of Grb2 was revealed in our assessment of its receptor-binding profile in the presence of ShcD Y1F through Y6F. As validated Grb2-binding motifs were removed from ShcD, endogenous Grb2 accumulated on TrkB, and Erk signaling resumed. Although Grb2 was previously thought to associate only indirectly with Trk receptors, two recognition motifs have since been identified in TrkA (26) that are conserved in TrkB. The co-immunoprecipitation patterns we observed are thus consistent with a stoichiometric partitioning hypothesis in which ShcD and TrkB compete to bind Grb2.

Intriguingly, the pErk super-suppressor effect arising from the ShcD SH2* mutation appears to align with the novel binding and functional relationship that we uncovered between ShcD and Shp2. This phosphatase is the first regulatory component that has been found to reduce ShcD CH1 region tyrosine phosphorylation and the only known partner that interacts primarily through the ShcD SH2 domain. The ShcD CH1 region phosphotyrosine motifs also appear to contribute somewhat to the Shp2 association, but it is yet unclear whether they independently engage a Shp2 SH2 domain or act in *cis* to prime the ShcD SH2 domain for interactions as has been shown for ShcA (27). Across the Shc family, PTB-mediated associations are considerably more common and serve to connect ShcA with a handful of phosphatases, including PTP-PEST, PP2A, and PTPϵ (2). However, the resulting ShcA dephosphorylation is traditionally associated with reduced MAPK activation in stark contrast to the inverse relationship we observed with ShcD whereby dephosphorylation leads to increased MAPK activation. In addition to this unique role in regulating ShcD CH1 motifs, Shp2 is already an established participant in neurotrophin signaling. The phosphatase complexes with active TrkB via fibroblast growth factor receptor substrate 2 and has been found to enable robust and prolonged MAPK activation following BDNF stimulation (28). Moreover, ShcA and fibroblast growth factor receptor substrate 2 compete for the same PTB-binding motif on Trk, which is speculated to determine whether stimuli provoke cellular proliferation or differentiation, respectively (29). The significance of Shp2 to neurotrophin-mediated MAPK activation suggests that the potent Erk

suppression elicited by ShcD-SH2* may arise not only from impeded Shp2-ShcD regulation, which impacts the Grb2 equilibrium, but also from competitive exclusion of Shp2 from the signaling complex as a whole. Breaking the interaction between Trk and Shp2 has indeed been associated with reduced MAPK activation (30). Our findings thus indicate that wild type ShcD controls recruitment and partitioning of multiple signal transduction components, including Grb2 and Shp2, and that the different receptor engagement strategies utilized by these factors establish distinct signaling fates. Indeed, although ShcA has been considered a molecular amplifier that sensitizes the cell to low levels of growth factor (31), ShcD may function as an integration hub, the output from which would depend on the nature and ratio of the recruited signal transducers.

The importance and centrality of MAPK/Erk signaling make it a prime candidate for regulation, and several proteins are tasked with this role within the cell (32). Select circumstances have even been identified in which Shc proteins inhibit the pathway. In the absence of stimuli, for example, the ShcA PTB domain can bind and suppress Erk until activating conditions are encountered that promote its release, thereby implicating ShcA in the prevention of spurious MAPK signaling (33). However, it is the response of the p66 ShcA isoform to stimulated EGFR that is perhaps most reminiscent of our observations with ShcD. Unlike p52 and p46 ShcA, p66 opposes Erk activation distal to the EGFR in a phenomenon that has been attributed to secondary p66 serine/threonine phosphorylation. In the context of ligand stimulation, p66 Ser/Thr phosphorylation is thought to destabilize the EGFR-Shc interaction, thereby uncoupling Grb2-son of sevenless (SOS) 1 from the receptor and deactivating the MAPK cascade (12, 13). In a variation on this theme, severe oxidative stress has been found to enhance the association of p66 with both EGFR and Grb2 while excluding SOS1 from the signaling complex (34). Stress-induced phosphorylation of residue Ser-36 on p66 ShcA appears to reduce the affinity of Grb2 for SOS1, effectively breaking the biochemical chain of command that activates Ras and eventually Erk (34). It therefore seems that ShcD is similar to p66 ShcA in its capacity to compete for a limited pool of Grb2 and direct it toward non-canonical outcomes, although it remains to be seen whether ShcD is likewise subject to serine/threonine-based regulation and whether this in turn influences the recruitment of SOS1. Intriguingly, Grb2 sequestration appears to be a common theme in MAPK modulation as this strategy is shared with the well characterized negative signaling regulators belonging to the Sprouty family (35).

Although further investigation is required to identify the broader physiological ramifications of non-canonical Shc behavior, there is a compelling precedent for Shc proteins to influence cellular outcomes based on MAPK activation pattern. Neuroblastoma tumors are unique in their capacity to spontaneously resolve in some young patients (36); however, TrkB and ShcC are both associated with negative prognoses (37, 38). *In vitro*, ShcA supports sustained Erk signaling leading to differentiation, whereas ShcC suppresses MAPK activation to drive tumorigenicity (39). Our discovery that ShcD regulates pErk in the murine brain coupled with evidence of its overexpression in melanomas (10) and gliomas (24) raises intriguing possibilities

that ShcD could be a mechanistic determinant in development and disease.

Experimental procedures

Plasmids

Full-length cDNA encoding full-length wild type human ShcD (BC033907) and point-mutated versions of the protein, including ShcD PTB* (R315Q), SH2* (R548K), and Y6F, were previously cloned into pcDNA3 vector (Invitrogen) with a carboxyl-terminal triple FLAG epitope (9). ShcD-FLAG with N-terminal GFP was described previously (24). Similarly, ShcD-PTB, ShcD-SH2, and ShcD-SH2* were previously cloned into pGEX-4T-1 as GST fusion constructs. Wild type and kinase-dead (K547A) TrkA and TrkB (kinase-dead K573A) of rat origin with N-terminal HA tags were expressed from the pCMX vector as described previously (19). Untagged Ret MEN2A and the kinase-dead variant (K758M) in the pJ7Ω vector were kindly provided by Dr. Rizaldy Scott (Northwestern University). Shp2 wild type and Cys-to-Ser mutant were generous gifts from Dr. Tomoko Takano (McGill University) (40).

Antibodies

The following antibodies were obtained commercially and used for immunoblotting analysis at the indicated dilutions (prepared with $1\times$ TBST ($10\times$ TBST: 0.02 M Tris, 0.15 M NaCl, 0.5% Tween 20): mouse anti-FLAG clone M2 at 1:1000 (F3165, Sigma-Aldrich), rabbit anti-Erk at 1:2000 (137F5, Cell Signaling Technology), rabbit anti-pErk at 1:1000 (Thr-202/Tyr-204; D13.14.4E, Cell Signaling Technology), rabbit anti-Akt at 1:1000 (C67E7, Cell Signaling Technology), rabbit anti-pAkt at 1:2000 (Ser-473; D9E, Cell Signaling Technology), rabbit anti-pShc at 1:1000 (Tyr-239/240; 24345, Cell Signaling Technology), rabbit anti-SH-PTP2 at 1:1000 (c-18; sc-280, lot number H1315, Santa Cruz Biotechnology), mouse anti-HA at 1:1000 (12CA5), rabbit anti-Ret at 1:1000 (C31B4, Cell Signaling Technology), rabbit anti-Trk (c-14; sc-11, lot number B2411, Santa Cruz Biotechnology), mouse anti-Grb2 at 1:1000 (lot number 16, Transduction Laboratories), and rabbit anti-ShcD raised in house against the ShcD C terminus (9). Horseradish peroxidase-conjugated goat anti-mouse and goat anti-rabbit secondary antibodies (Bio-Rad) were used for immunoblotting detection.

Cell culture and lysis

HEK 293T cells obtained from the American Type Culture Collection (Manassas, VA) were grown in Dulbecco's modified Eagle's medium (DMEM) (Sigma-Aldrich) supplemented with 10% fetal bovine serum (FBS) and with 200 units/ml penicillin and 200 μg/ml streptomycin (Invitrogen) and maintained at 37 °C incubation with 5% CO_2. Cells were transfected using polyethylenimine (PEI) for 24–48 h and starved in serum free DMEM overnight prior to lysis. Cells were then washed with 5 ml of chilled phosphate-buffered saline (PBS; pH 7.4) and lysed in 900 μl of phospholipase C (PLC) plus buffer (10% glycerol, 50 mM Hepes, 150 mM NaCl, 1.5 mM $MgCl_2$, 1 mM EGTA, 10 mM NaPP$_i$, 100 mM NaF, and 1% Triton X-100) supplemented with 10 μg/ml aprotinin, 10 μg/ml leupeptin, 1 mM sodium

orthovanadate, and 1 mM phenylmethylsulfonyl fluoride (PMSF). Lysates were centrifuged at 12,000 $\times$ g, and the supernatant was removed and stored as whole-cell lysate (WCL) at -20 °C.

Immunoprecipitation and GST pulldown assays

Immunoprecipitation was performed overnight with rocking at 4 °C using 400 μl of WCL, primary antibody, and 10% anti-mouse IgG-agarose beads (Sigma) in a total volume of 800 μl of PLC plus buffer. Following removal of supernatant, beads were washed three times with 800 μl of PLC plus buffer, and protein complexes were eluted in $2\times$ SDS loading buffer by boiling at 100 °C for 3 min. GST fusion proteins for ShcD-PTB, ShcD-SH2, and disabled ShcD-SH2 (SH2*) were expressed in *Escherichia coli* BL21 cells by overnight induction with 0.5 mM isopropyl β-D-1-thiogalactopyranoside and purified using glutathione-Sepharose™ 4B beads (GE Healthcare). Purified GST fusion proteins (5 μg) were incubated with lysates overnight at 4 °C with rocking and processed as described for immunoprecipitation.

Immunoblotting

WCLs were used to prepare samples for separation on sodium dodecyl sulfate-polyacrylamide gel electrophoresis (SDS-PAGE) by diluting 80 μl of WCL in 20 μl of $5\times$ SDS loading buffer (50% glycerol, 300 mM Tris, 10% SDS, and 25% β-mercaptoethanol) and boiling at 100 °C for 2 min. For Western blotting, proteins from WCLs were resolved on a 10% SDS-polyacrylamide gel to separate proteins based on their molecular mass in kDa and then transferred to polyvinylidene fluoride (PVDF) membranes using semidry transfer. Membranes were blocked for 30 min in $1\times$ TBST diluted with sterile water containing 5% PBS and incubated overnight with primary antibody. Following the overnight incubation, the membranes were washed three times for 8–10 min in $1\times$ TBST and incubated with secondary antibody for 1 h at room temperature. Immunoblotting detection was performed using ECL Western blotting substrate (Pierce) and exposing the membranes to film (Pierce).

Densitometry and statistics

To determine relative immunoblot band intensities, membranes were imaged and quantitated using ImageLab analysis software (versions 2.0–5.2, Bio-Rad).

All statistical calculations were performed and plotted in GraphPad Prism version 7.0. Randomized block immunoblot replicate panels (minimum $n = 3$) were analyzed by repeated measures one-way ANOVA when data passed the Shapiro-Wilk normality test. Tukey's multiple comparison test was used to assess each condition against all other conditions and generate multiplicity-adjusted p values for significant pairs. A paired t test was used to compare signaling outcomes of wild type and knock-out mouse littermates.

Affinity purification-mass spectrometry

HEK 293T cells were transiently transfected with GFP-ShcD-FLAG or GFP-FLAG using PEI for 36 h and stimulated with 100 μM pervanadate for 20 min before lysis. Cleared lysates

were immunoprecipitated with anti-FLAG M2 affinity gel (Sigma-Aldrich) for 2 h at 4 °C before being processed for tryptic digestion as described previously (41). A 5600+ mass spectrometer equipped with a nanoelectrospray ion source (AB Sciex) and coupled to reversed-phase nanoscale capillary liquid chromatography with an Ekspert NanoLC425 (Eksigent) was used for peptide analysis. Mass spectra were acquired using a data-dependent acquisition mode with Analyst software (version 1.7, AB Sciex). All MS/MS peak lists were generated and set up to search the UniProt *Homo sapiens* database (March 2014 release, 69,150 entries) with fragment and parent ion mass tolerances of 0.100 Da. Scaffold (version 4.0.1, Proteome Software Inc.) was used to validate MS/MS-based peptide and protein identifications, which were accepted if they contained at least one identified peptide and could be established at greater than 99.0% probability to achieve a false discovery rate of less than 1.0%. Proteins that contained similar peptides and that could not be differentiated based on MS/MS analysis alone were grouped to satisfy the principles of parsimony. Experiments were performed in triplicate. MS data were analyzed with SAINTexpress, a simplified version of the Significance Analysis of INTeractome method described previously (42) via the CRAPome website (43). SAINT probabilities were calculated using MS data from GFP-FLAG as controls to distinguish ShcD-specific interactors from background. Ptpn11/Shp2 was assigned a perfect score of 1.0.

ShcD knock-out mice

A homologous recombination/Cre excision strategy was used to conditionally delete exon 7 in the *ShcD* gene and generate full body ShcD knock-out mice.[10] Female mice at ~1 year of age were used in this study (*n* = 3 per genotype). Freshly isolated brain tissue was lysed in PLC plus buffer using a Dounce homogenizer, and lysate was cleared by centrifugation prior to protein concentration determination by BCA assay (Thermo Scientific). 100 μg of total cell lysate was loaded for Western analysis. Animal studies were carried out in accordance with Canadian Council on Animal Care protocols.

References

1. Pawson, T., and Scott, J. D. (1997) Signaling through scaffold, anchoring, and adaptor proteins. *Science* **278,** 2075–2080
2. Wills, M. K., and Jones, N. (2012) Teaching an old dogma new tricks: twenty years of Shc adaptor signalling. *Biochem. J.* **447,** 1–16
3. Ponti, G., Reitano, E., Aimar, P., Cattaneo, E., Conti, L., and Bonfanti, L. (2010) Neural-specific inactivation of ShcA functions results in anatomical disorganization of subventricular zone neural stem cell niche in the adult brain. *Neuroscience* **168,** 314–322
4. Ponti, G., Conti, L., Cataudella, T., Zuccato, C., Magrassi, L., Rossi, F., Bonfanti, L., and Cattaneo, E. (2005) Comparative expression profiles of ShcB and ShcC phosphotyrosine adapter molecules in the adult brain. *Neuroscience* **133,** 105–115
5. Villanacci, V., Bassotti, G., Ortensi, B., Fisogni, S., Cathomas, G., Maurer, C. A., Galletti, A., Salerni, B., and Pelicci, G. (2008) Expression of the Rai (Shc C) adaptor protein in the human enteric nervous system. *Neurogastroenterol. Motil.* **20,** 206–212
6. Ferro, M., Savino, M. T., Ortensi, B., Finetti, F., Genovese, L., Masi, G., Ulivieri, C., Benati, D., Pelicci, G., and Baldari, C. T. (2011) The Shc family protein adaptor, Rai, negatively regulates T cell antigen receptor signaling by inhibiting ZAP-70 recruitment and activation. *PLoS One* **6,** e29899
7. Savino, M. T., Ortensi, B., Ferro, M., Ulivieri, C., Fanigliulo, D., Paccagnini, E., Lazzi, S., Osti, D., Pelicci, G., and Baldari, C. T. (2009) Rai acts as a negative regulator of autoimmunity by inhibiting antigen receptor signaling and lymphocyte activation. *J. Immunol.* **182,** 301–308
8. Hawley, S. P., Wills, M. K., Rabalski, A. J., Bendall, A. J., and Jones, N. (2011) Expression patterns of ShcD and Shc family adaptor proteins during mouse embryonic development. *Dev. Dyn.* **240,** 221–231
9. Jones, N., Hardy, W. R., Friese, M. B., Jorgensen, C., Smith, M. J., Woody, N. M., Burden, S. J., and Pawson, T. (2007) Analysis of a Shc family adaptor protein, ShcD/Shc4, that associates with muscle-specific kinase. *Mol. Cell. Biol.* **27,** 4759–4773
10. Fagiani, E., Giardina, G., Luzi, L., Cesaroni, M., Quarto, M., Capra, M., Germano, G., Bono, M., Capillo, M., Pelicci, P., and Lanfrancone, L. (2007) RaLP, a new member of the Src homology and collagen family, regulates cell migration and tumor growth of metastatic melanomas. *Cancer Res.* **67,** 3064–3073
11. Gertz, M., and Steegborn, C. (2010) The lifespan-regulator p66Shc in mitochondria: redox enzyme or redox sensor? *Antioxid. Redox Signal.* **13,** 1417–1428
12. Okada, S., Kao, A. W., Ceresa, B. P., Blaikie, P., Margolis, B., and Pessin, J. E. (1997) The 66-kDa Shc isoform is a negative regulator of the epidermal growth factor-stimulated mitogen-activated protein kinase pathway. *J. Biol. Chem.* **272,** 28042–28049
13. Migliaccio, E., Mele, S., Salcini, A. E., Pelicci, G., Lai, K. M., Superti-Furga, G., Pawson, T., Di Fiore, P. P., Lanfrancone, L., and Pelicci, P. G. (1997) Opposite effects of the p52shc/p46shc and p66shc splicing isoforms on the EGF receptor-MAP kinase-fos signalling pathway. *EMBO J.* **16,** 706–716
14. Conti, L., Sipione, S., Magrassi, L., Bonfanti, L., Rigamonti, D., Pettirossi, V., Peschanski, M., Haddad, B., Pelicci, P., Milanesi, G., Pelicci, G., and Cattaneo, E. (2001) Shc signaling in differentiating neural progenitor cells. *Nat. Neurosci.* **4,** 579–586
15. Ledda, F., and Paratcha, G. (2016) Assembly of neuronal connectivity by neurotrophic factors and leucine-rich repeat proteins. *Front. Cell. Neurosci.* **10,** 199
16. Reichardt, L. F. (2006) Neurotrophin-regulated signalling pathways. *Philos. Trans. R. Soc. Lond. B Biol. Sci.* **361,** 1545–1564
17. Sariola, H., and Saarma, M. (2003) Novel functions and signalling pathways for GDNF. *J. Cell Sci.* **116,** 3855–3862
18. Allen, S. J., and Dawbarn, D. (2006) Clinical relevance of the neurotrophins and their receptors. *Clin. Sci.* **110,** 175–191
19. Liu, H.-Y., and Meakin, S. O. (2002) ShcB and ShcC activation by the Trk family of receptor tyrosine kinases. *J. Biol. Chem.* **277,** 26046–26056
20. Pelicci, G., Troglio, F., Bodini, A., Melillo, R. M., Pettirossi, V., Coda, L., De Giuseppe, A., Santoro, M., and Pelicci, P. G. (2002) The neuron-specific Rai (ShcC) adaptor protein inhibits apoptosis by coupling Ret to the phosphatidylinositol 3-kinase/Akt signaling pathway. *Mol. Cell. Biol.* **22,** 7351–7363
21. Knauf, J. A., Kuroda, H., Basu, S., and Fagin, J. A. (2003) RET/PTC-induced dedifferentiation of thyroid cells is mediated through Y1062 signaling through SHC-RAS-MAP kinase. *Oncogene* **22,** 4406–4412
22. Smith, M. J., Hardy, W. R., Murphy, J. M., Jones, N., and Pawson, T. (2006) Screening for PTB domain binding partners and ligand specificity using proteome-derived NPXY peptide arrays. *Mol. Cell. Biol.* **26,** 8461–8474

23. You, Y., Li, W., Gong, Y., Yin, B., Qiang, B., Yuan, J., and Peng, X. (2010) ShcD interacts with TrkB via its PTB and SH2 domains and regulates BDNF-induced MAPK activation. *BMB Rep.* **43,** 485–490

24. Wills, M. K., Tong, J., Tremblay, S. L., Moran, M. F., and Jones, N. (2014) The ShcD signaling adaptor facilitates ligand-independent phosphorylation of the EGF receptor. *Mol. Biol. Cell.* **25,** 739–752

25. Santoro, M., Carlomagno, F., Romano, A., Bottaro, D. P., Dathan, N. A., Grieco, M., Fusco, A., Vecchio, G., Matoskova, B., and Kraus, M. H. (1995) Activation of RET as a dominant transforming gene by germline mutations of MEN2A and MEN2B. *Science* **267,** 381–383

26. MacDonald, J. I., Gryz, E. A., Kubu, C. J., Verdi, J. M., and Meakin, S. O. (2000) Direct binding of the signaling adapter protein Grb2 to the activation loop tyrosines on the nerve growth factor receptor tyrosine kinase, TrkA. *J. Biol. Chem.* **275,** 18225–18233

27. George, R., Schuller, A. C., Harris, R., and Ladbury, J. E. (2008) A phosphorylation-dependent gating mechanism controls the SH2 domain interactions of the Shc adaptor protein. *J. Mol. Biol.* **377,** 740–747

28. Easton, J. B., Royer, A. R., and Middlemas, D. S. (2006) The protein tyrosine phosphatase, Shp2, is required for the complete activation of the RAS/MAPK pathway by brain-derived neurotrophic factor. *J. Neurochem.* **97,** 834–845

29. Meakin, S. O., MacDonald, J. I., Gryz, E. A., Kubu, C. J., and Verdi, J. M. (1999) The signaling adapter FRS-2 competes with Shc for binding to the nerve growth factor receptor TrkA. A model for discriminating proliferation and differentiation. *J. Biol. Chem.* **274,** 9861–9870

30. Kumamaru, E., Numakawa, T., Adachi, N., and Kunugi, H. (2011) Glucocorticoid suppresses BDNF-stimulated MAPK/ERK pathway via inhibiting interaction of Shp2 with TrkB. *FEBS Lett.* **585,** 3224–3228

31. Lai, K. M., and Pawson, T. (2000) The ShcA phosphotyrosine docking protein sensitizes cardiovascular signaling in the mouse embryo. *Genes Dev.* **14,** 1132–1145

32. McKay, M. M., and Morrison, D. K. (2007) Integrating signals from RTKs to ERK/MAPK. *Oncogene* **26,** 3113–3121

33. Suen, K. M., Lin, C.-C., George, R., Melo, F. A., Biggs, E. R., Ahmed, Z., Drake, M. N., Arur, S., Arold, S. T., and Ladbury, J. E. (2013) Interaction with Shc prevents aberrant Erk activation in the absence of extracellular stimuli. *Nat. Struct. Mol. Biol.* **20,** 620–627

34. Arany, I., Faisal, A., Nagamine, Y., and Safirstein, R. L. (2008) p66shc inhibits pro-survival epidermal growth factor receptor/ERK signaling during severe oxidative stress in mouse renal proximal tubule cells. *J. Biol. Chem.* **283,** 6110–6117

35. Hanafusa, H., Torii, S., Yasunaga, T., and Nishida, E. (2002) Sprouty1 and Sprouty2 provide a control mechanism for the Ras/MAPK signalling pathway. *Nat. Cell Biol.* **4,** 850–858

36. Brodeur, G. M. (2003) Neuroblastoma: biological insights into a clinical enigma. *Nat. Rev. Cancer* **3,** 203–216

37. Brodeur, G. M., Minturn, J. E., Ho, R., Simpson, A. M., Iyer, R., Varela, C. R., Light, J. E., Kolla, V., and Evans, A. E. (2009) Trk receptor expression and inhibition in neuroblastomas. *Clin. Cancer Res.* **15,** 3244–3250

38. Terui, E., Matsunaga, T., Yoshida, H., Kouchi, K., Kuroda, H., Hishiki, T., Saito, T., Yamada, S., Shirasawa, H., and Ohnuma, N. (2005) Shc family expression in neuroblastoma: high expression of shcC is associated with a poor prognosis in advanced neuroblastoma. *Clin. Cancer Res.* **11,** 3280–3287

39. Miyake, I., Ohira, M., Nakagawara, A., and Sakai, R. (2009) Distinct role of ShcC docking protein in the differentiation of neuroblastoma. *Oncogene* **28,** 662–673

40. Aoudjit, L., Jiang, R., Lee, T. H., New, L. A., Jones, N., and Takano, T. (2011) Podocyte protein, nephrin, is a substrate of protein tyrosine phosphatase 1B. *J. Signal Transduct.* **2011,** 376543

41. Beigbeder, A., Vélot, L., James, D. A., and Bisson, N. (2016) Sample preparation for mass spectrometry analysis of protein-protein interactions in cancer cell lines and tissues. *Methods Mol. Biol.* **1458,** 339–347

42. Teo, G., Liu, G., Zhang, J., Nesvizhskii, A. I., Gingras, A.-C., and Choi, H. (2014) SAINTexpress: improvements and additional features in Significance Analysis of INTeractome software. *J. Proteomics* **100,** 37–43

43. Mellacheruvu, D., Wright, Z., Couzens, A. L., Lambert, J.-P., St-Denis, N. A., Li, T., Miteva, Y. V., Hauri, S., Sardiu, M. E., Low, T. Y., Halim, V. A., Bagshaw, R. D., Hubner, N. C., Al-Hakim, A., Bouchard, A., *et al.* (2013) The CRAPome: a contaminant repository for affinity purification-mass spectrometry data. *Nat. Methods* **10,** 730–736